Available online at www.sciencedirect.com
SCIENCE DIRECT®
Real-Time Imaging 9 (2003) 245–251
www.elsevier.com/locate/rti

Real-time classification of polymers with NIR spectral imaging and blob analysis

R. Leitner*, H. Mairer, A. Kercek

Carinthian Tech Research AG, Europastrasse 4/1, A-9524 Villach/St. Magdalen, Austria

Abstract

Near-infrared (NIR) spectroscopy is widely used in laboratory and industrial applications for material classification. While standard spectrometers only allow measurement at one sampling point at a time, NIR Spectral Imaging techniques can identify, in real-time, both the size and shape of an object as well as the material it is made from. The robust classification of materials, such as polymers, is based on their characteristic reflectance spectra. As a sample application, we present the real-time classification of waste polymers in a prototype of an automated industrial sorting facility. Sorting requires the correct material, size and shape of the entire object to be known for reliable separation. In this paper, a method for paper label detection on polymer parts is introduced, aimed at enhancing the classification results by merging connected parts of an object.

1. Introduction

Near-infrared (NIR) spectroscopy is a widely used analytical tool, both in laboratory and field applications [1,2]. A number of NIR process analysers are commercially available, but these instruments are usually confined to point analysis. With the advent of direct sight imaging spectrographs [3], Spectral Imaging systems capable of acquiring hundreds of spectra with high spectral and high spatial resolution at the frame speed of standard cameras are available, thus making real-time classification systems feasible [4].

Spectral imaging (SI) is the combination of spectroscopy with digital image processing [5–7]. While the images produced by conventional digital cameras contain the intensity, or some colour channels (e.g. RGB), of single image pixels, SI provides the full spectral information for each pixel over a selected wavelength range. In instrumentation there are two approaches: the first approach is the wavelength scanning method, in remote sensing also known as "staring imagers". Single images are recorded for each different wavelength, while the sample is kept stationary under the SI camera. Three general approaches exist to provide the spectral information: (i) a number of discrete filters [8], (ii) tuneable filters [9] or (iii) with an imaging Fourier-Transform spectrometer [10,11]. The images recorded for the different wavelengths are combined in the computer, allowing the calculation of the spectrum for each pixel. The second approach requires a relative movement between imager and sample to scan over the surface. The Spectral Imaging system records the spatial information line-wise, and the spectrum for each pixel along the line is projected along the second axis of the two-dimensional camera chip. The spectral encoding is provided either by linearly variable filters [12] or by dispersive optics forming an imaging spectrograph [13]. A computer combines the slices, derives the second axis and thus reconstructs the full image. Such an imaging spectrograph based on dispersive optics was chosen as most suitable for our application.

Imaging spectrographs are available for different wavelength ranges from UV to IR and a suitable range for polymer classification has to be selected. The NIR region, in particular the range from 1000 to 1700 nm provides sufficient material specific information—due to overtone and combination vibrational absorption bands—to make a reliable classification while still being accessible with standard optics.

Spectral Imaging systems have been used in a number of applications, showing the applicability of spectral data for material classification and inspection, but real-time requirements, which are of key importance

*Corresponding author. Tel.: +43-4242-56300; fax: +43-4242-56300.
E-mail address: raimund.leitner@ctr.at (R. Leitner).
URL: http://www.ctr.at.

1077-2014/$ - see front matter © 2003 Elsevier Ltd. All rights reserved.
doi:10.1016/j.rti.2003.09.016

for industrial applications, have rarely been taken into account. Examples for such applications can be found in e.g. (i) the food industry, for fruit quality and ripeness control during and after harvesting [14,15] or for the detection of contamination on poultry [16], (ii) for general colour measurements [17], or (iii) for geological and mineralogical applications, e.g. the discrimination of natural and artificial turquoises [18].

2. Prototype system

The laboratory-scale system (Fig. 1) consists of an imaging spectrograph (ImSpector N17, Specim Ltd., Finland) with a spectral range of 900–1700 nm and a spectral resolution of 13 nm. The ImSpector consists of a prism–grating–prism arrangement dispersing the radiation coming through an 80 μm slit. The resulting 2D image represents the light intensities along the observation line (first spatial axis) and the wavelength axis. This image is acquired with a spectrally matched InGaAs camera (SU320-1.7RT, Sensors Unlimited Inc., USA) with a spectral range from 900 to 1700 nm and a nominal resolution of 320×240 pixels. An NIR optimised lens is attached to the front of the spectrograph, governing the resolution and the field of view in the first spatial axis.

A conveyor belt below the camera moves the samples at a constant speed, perpendicular to the observation line. By combining consecutively acquired frames in the computer, the second spatial dimension is obtained. The velocity of the conveyor belt and the frame-rate of the camera determine the resolution in the second spatial axis. Each frame acquired by the laboratory-scale system records the spectral information of a rectangular area of 600 mm × 1.4 mm on the conveyor belt.

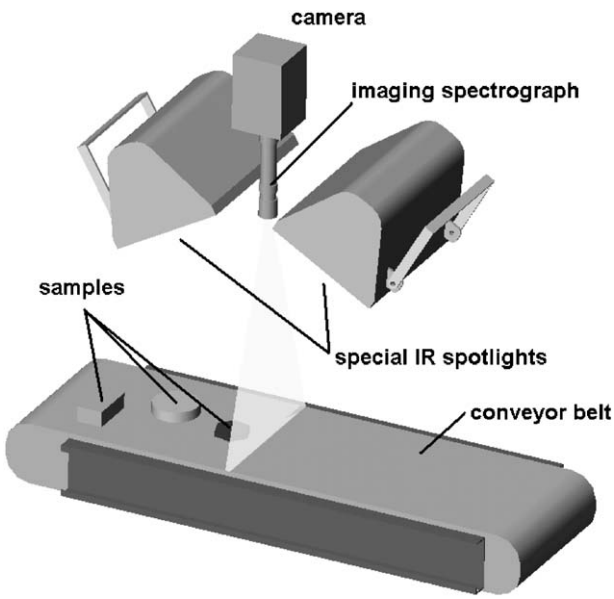

Fig. 1. Laboratory-scale system.

To achieve sufficient light intensity for reflection measurements in the NIR, the samples are illuminated with four 350 W infrared-enhanced spotlights, located before and after the imaging spectrograph. Special diffusing glasses are mounted on the spotlights to give homogeneous illumination in the field of view.

3. Pre-processing

The raw images acquired by the camera have to be pre-processed to correct for the measurement deficiencies of the acquisition system and to reduce the amount of data for an efficient real-time classification. There are two corrections: (i) a dark current correction (dark-current image $B(x,\lambda)$) and (ii) a detector calibration, performed by measuring a white diffuse reflectance standard (white-standard image $W(x,\lambda)$). The final reflectance images $R(x,\lambda)$ are calculated from the sample image $X(x,\lambda)$ and the two compensation images $B(x,\lambda)$ and $W(x,\lambda)$ according to Eq. (1).

$$R(x,\lambda) = \frac{X(x,\lambda) - B(x,\lambda)}{W(x,\lambda) - B(x,\lambda)}. \quad (1)$$

The resolution of the InGaAs camera is higher than the ImSpector's resulting in redundant data. The camera delivers images with 320×240 pixels, which are reduced to 80×240 pixels by Gaussian averaging and binning in the wavelength direction. The resulting reflectance images have a resolution of 80 (spectral) × 240 (spatial) pixels. These are arranged as 240 vectors with 80 elements, where each vector corresponds to one spectrum.

4. Classification

4.1. Classification algorithms

Most technical polymers can be distinguished by their characteristic absorption bands in the NIR. In the experimental range between 1000 and 1700 nm the second overtone C–H stretching and the C–H combination bands are particularly useful. Preliminary experiments have proved that a robust real time classification of most technical polymers is feasible with NIR spectral imaging [4]. Fig. 2 shows the characteristic spectra of four common polymers: high-density polyethylene (HDPE), two types of polypropylene (PP Cup, PP Bottle), polystyrene (PS), and polyethylene terephthalate (PET).

The material specific features of the spectra are the rising and falling slopes of the different absorption bands, while the absolute intensities contain significantly less discriminative information. By using differentiated

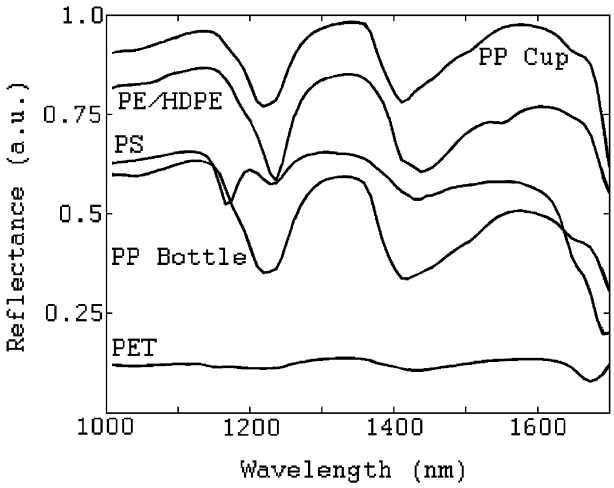

Fig. 2. Sample spectra of five polymers.

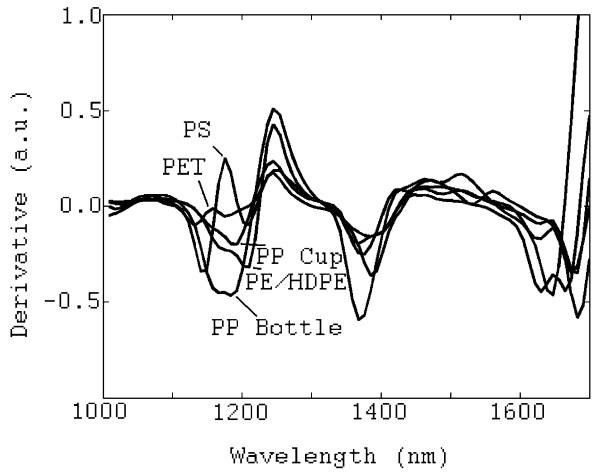

Fig. 3. Normalized and differentiated spectra of five common waste polymers.

spectra as input for the classification the material specific features are enhanced. Fig. 3 shows the differentiated spectra of the polymers displayed in Fig. 2.

Three potentially suitable classifiers have been evaluated off-line using Matlab® (The Mathworks Inc., USA) and a proprietary spectral imaging toolbox (CTR AG, Austria).

4.1.1. Fisher linear discriminant classifier

Fisher linear discriminant classifier (FLDC) performs a linear mapping to a lower dimensional subspace, which is optimised for class separability, prior to the classification using a linear classifier. During training the mapping $\mathbf{w}$ is optimized for class separability in the subspace by maximizing the criterion

$$J(\mathbf{w}) = \frac{\mathbf{w}^t S_B \mathbf{w}}{\mathbf{w}^t S_W \mathbf{w}} \tag{2}$$

with the between-class scatter S_B and the within-class scatter S_W. For c classes the mapping projects the input data on a subspace with $c-1$ dimensions, often called Fisher scores, and subsequently a conventional linear discriminant classifier is trained on the Fisher scores. The log-likelihood is calculated by

$$\ln(p(\mathbf{x})) = -\frac{(\mathbf{x}-\mu)^T G^{-1}(\mathbf{x}-\mu)}{2} + const \tag{3}$$

with the estimated covariance matrix over all classes G and the class mean μ. Each sample is assigned to the class giving the highest log-likelihood.

4.1.2. Quadratic discriminant classifier

In contrast to a linear discriminant classifier, QDC estimates mean and covariance for each class, allowing the classifier to find more suitable discriminant functions. If QDC is applied directly to the data, eventually some of the covariance matrices become singular due to correlations in the spectral data. Using principal component analysis (PCA) the input data can be reduced to typically 10 principal components, which retain the significant variance and give better covariance matrices. During training, the probability density functions of the individual training classes in the principal component space are estimated from the training data. Normally distributed data are assumed, and the distribution parameters (sample mean and covariance) are estimated with maximum-likelihood estimation. Each sample is assigned to the class with the highest log-likelihood calculated following Eq. (4) with the class mean μ and class covariance Σ.

$$\ln(p(\mathbf{x})) = -\frac{(\mathbf{x}-\mu)^T \Sigma^{-1}(\mathbf{x}-\mu)}{2} - \frac{1}{2}\ln(\det \Sigma) + const. \tag{4}$$

4.1.3. Dissimilarity-based classifier

DBC [19] use a dissimilarity measure M_D to transform the input data into a dissimilarity space, where each training prototype represents a separate dimension. Any dissimilarity measure with following properties can be used:

$$M_D(\mathbf{x},\mathbf{y}) = \left\{ \begin{array}{ll} 0, & \mathbf{x}=\mathbf{y} \\ >0, & \mathbf{x}\neq\mathbf{y} \end{array} \right\}. \tag{5}$$

By designing the dissimilarity measure, it is possible to use expert knowledge or application dependent properties to construct an efficient dissimilarity space, where classification is often easier than in the original feature space. For the classification of spectra, the *Euclidian distance*, the *cumulative sum of spectral differences* and *geometric measures* proved to be useful discriminative dissimilarity measures.

Generally, a certain number of random samples are used as class prototypes for DBC. We use a special form

of a DBC, which will be referred as DBC-NN, using a nearest neighbour classifier and a single class prototype. The class prototype is computed from the average spectrum of manually selected regions from the training data. The same manually selected regions served as the training input for all three classifiers to ensure a fair comparison. The results support that a single class prototype is sufficient for reliable polymer classification.

4.2. Runtime complexity

For real-time applications the execution time of the algorithm is crucial. The execution time depends mainly on the number of significant operations (multiplications, additions) of the algorithm and in the following discussion we use the O-notation for the asymptotic upper bound of an algorithm's complexity. Although the vector and matrix dimensions are finite and rather small, the O-notation is a good indicator for the behaviour of the execution time for the real-time application. The number of elements in each vector (spectrum) is denoted by n, the elements after the Fisher mapping or PCA-transformation by m and the number of classes by p. The inverse and the determinant of the covariance matrices for FLDC and QDC can be calculated during pre-processing and hence do not contribute to the computational complexity.

The required operations to classify a single sample spectrum are considered for each classifier. The linear mapping and the PCA-transformation both correspond to a vector-matrix multiplication with the complexity of $O(nm)$. The computational complexity of the FLDC is $O(nm)$ for the linear mapping and $O(pm^2)$ for the vector-matrix-vector multiplication for each class, giving a complexity of $O(nm + pm^2)$. QDC requires also $O(nm + pm^2)$ operations like the FLDC (the logarithm of the determinant can be obtained in constant time), hence FLDC and QDC (with PCA) are equal with respect to computational complexity. The computational complexity of DBC-NN is $O(jp)O_M$ with O_M, j, and p denoting the runtime complexity of the dissimilarity measure, the number of class prototypes and the number of classes, respectively. The used dissimilarity measures in our experiments require $O(n)$ operations, giving $O(jpn)$ operations for DBC-NN. For larger numbers (especially the number of classes) the DBC-NN achieves a computational advantage over FLDC and QDC, but using the actual values of the proposed polymer classification the difference between FLDC and DBC-NN is rather small (Table 1).

Table 1
Runtime complexity of the classifiers

Classifier	Runtime complexity	Polymer classification
Fisher linear discriminant classifier	$O(nm + pm^2)$	$O(550)$
PCA and quadratic discriminant classifier	$O(nm + pm^2)$	$O(1400)$
Dissimilarity-based classifier (DBC-NN)	$O(jpn)$	$O(480)$

The number of input features, the number of features after Fisher mapping or PCA, the number of class prototypes, and the number of classes are denoted by n, m, j, and p, respectively.

4.3. Classification results

The classifiers were evaluated on a test set containing several waste polymers. The training set was composed from 10% randomly chosen sample spectra from the test set and was excluded from the test set for the performance evaluation. Table 2 shows the classifier set-up for the performance evaluation with number of features for each classifier and percentage of correct classified sample spectra. The performance percentage is the ratio of correctly classified samples to samples with ground truth. FLDC and QDC classified some bottle caps and dark and bright regions wrongly, while DBC-NN achieves the best performance rating and also classifies the caps correctly. The correct classification of caps is important for polymer recycling applications, because caps (e.g. PE) are often made of different materials than bottles (e.g. PET) and could contaminate the target fractions, if the classification does not report them correctly.

Table 2
Classifier set-up and the number of features for the three evaluated classifiers, the number of features after the Fisher mapping or PCA and the performance on the test set with waste polymers (84315 sample spectra, 10% were used for training)

Classification	Input features	Class features	Performance (%)
Fisher linear discriminant classifier	80	5	53.89
PCA and quadratic discriminant classifier	80	10	88.16
Dissimilarity-based classifier (DBC-NN)	80	80	93.41

The spectra exhibit large in-class variation, due to many factors such as sample variation, illumination differences, object surface properties, etc. The statistical classifiers like FLDC and QDC are not able to capture all these variations completely resulting in a poor performance. The ability of the dissimilarity-based classifier (DBC-NN) to generalize makes it more suitable for spectral classification than the statistically more powerful FLDC and QDC.

DBC-NN achieves the best performance of the evaluated classifiers and is also suitable for real-time

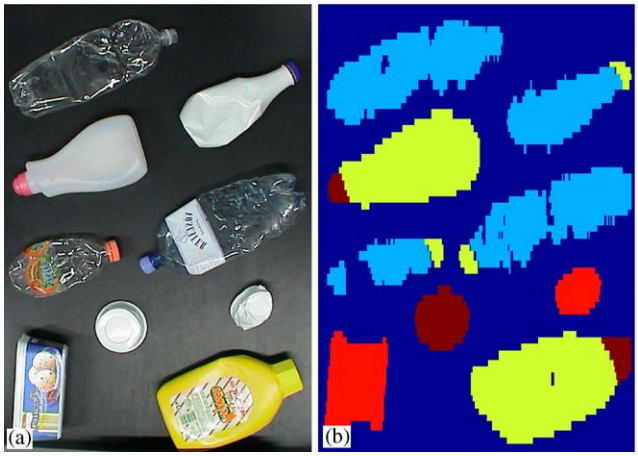

Fig. 4. Digital RGB image (a) and enhanced classification result (scaled) obtained with the proposed real-time system (b) the colour mapping is light blue for PET, green for PE, red for PS and brown for PP. The colour mapping is the same as for Fig. 5(a)–(c).

classification. Consequently, DBC-NN was chosen for the real-time classification system and implemented in C++. The real-time classification system implemented in C++ was tested on a standard PC and achieved the full frame rate of the camera (50 frames per second) with the proposed pre-processing and classification algorithms. Fig. 4 shows an RGB image of waste polymers and the classification result obtained with the real-time classification system (the classification result has been rescaled to visualize the correct correspondences).

5. Blob analysis—label detection

The classifier estimates the material class of each pixel, providing a spatial image indicating the material. Image-processing techniques can be applied to enhance the classification result. Industrial applications require a reliable material classification of an entire object, e.g. a PET bottle with a paper label should be detected as one single PET object, since a subsequent sorting or turnout stage has to handle entire objects based on the classification result. This requires that a classification system delivers the correct size and shape of the different objects, regardless of the presence of other materials e.g. paper labels, which partially obscure the objects' surfaces.

To get an initial estimate for object reconstruction, connected components (blobs) are detected in the binary images of each material class. Blobs that do not meet pre-defined size restrictions are considered as classification errors and filtered out.

The proposed procedure detects paper labels on objects and merges the object and label into a single object indicating the real contours of the object. This enhances the classification result considerably and increases the performance of the subsequent turnout stage. The binary image of each material class (polymer and paper) is morphologically dilated with a box mask (3×3) and the dilated paper blobs are overlaid with the dilated blobs of each polymer class to detect overlaps (logical "AND"). These overlaps identify regions in the classification result where polymer and paper regions touch each other. Adjacent regions will be merged to a single blob, if one of the following two conditions is fulfilled:

C1: the centre of the paper blob and the polymer blob lie inside a circle with a certain diameter.
C2: the centre of the paper blob lies between two polymer blobs.

Fig. 5 shows the original classification result (a), the dilated classification result (b) with the overlap regions (orange, cyan) and the enhanced classification result (c). The black marks indicate the individual blob centres.

The first merging condition (C1) is used for the object in the lower right of Fig. 5(b). Here, the paper label is enclosed by the polymer material, allowing both blobs to be merged. The middle right object in Fig. 5(b) illustrates the second merging condition (C2) for a PET-bottle with a paper label, which separates the polymer blob into two regions.

The classification delivers the classification result of a pixel-line each frame. For an efficient real-time solution, the pixel-lines are accumulated to a running history of 50 pixel-lines in a circular buffer, which is updated at the acquisition of each frame. For each frame only a single pixel-line is removed, a new line added and the remaining lines are shifted accordingly, thus enabling a continuous real-time blob analysis. The overlap needs to be updated only for the single new line and the blob centres have to be re-calculated to reflect the changes.

6. Conclusion

We have shown that Spectral Imaging is a valuable method for on-line, real-time classification of synthetic polymers based directly on the material properties. Best performance in terms of pixel-wise classification is achieved with the dissimilarity-based classifier (DBC-NN), which classified over 93% of the sample spectra correctly.

The proposed algorithms allow the reliable removal of paper labels from the classification result. Hence it is possible to classify the entire object correctly according to its material using a priori knowledge about the objects.

Spectral Imaging combined with dissimilarity-based classifiers and object-directed post-processing is a

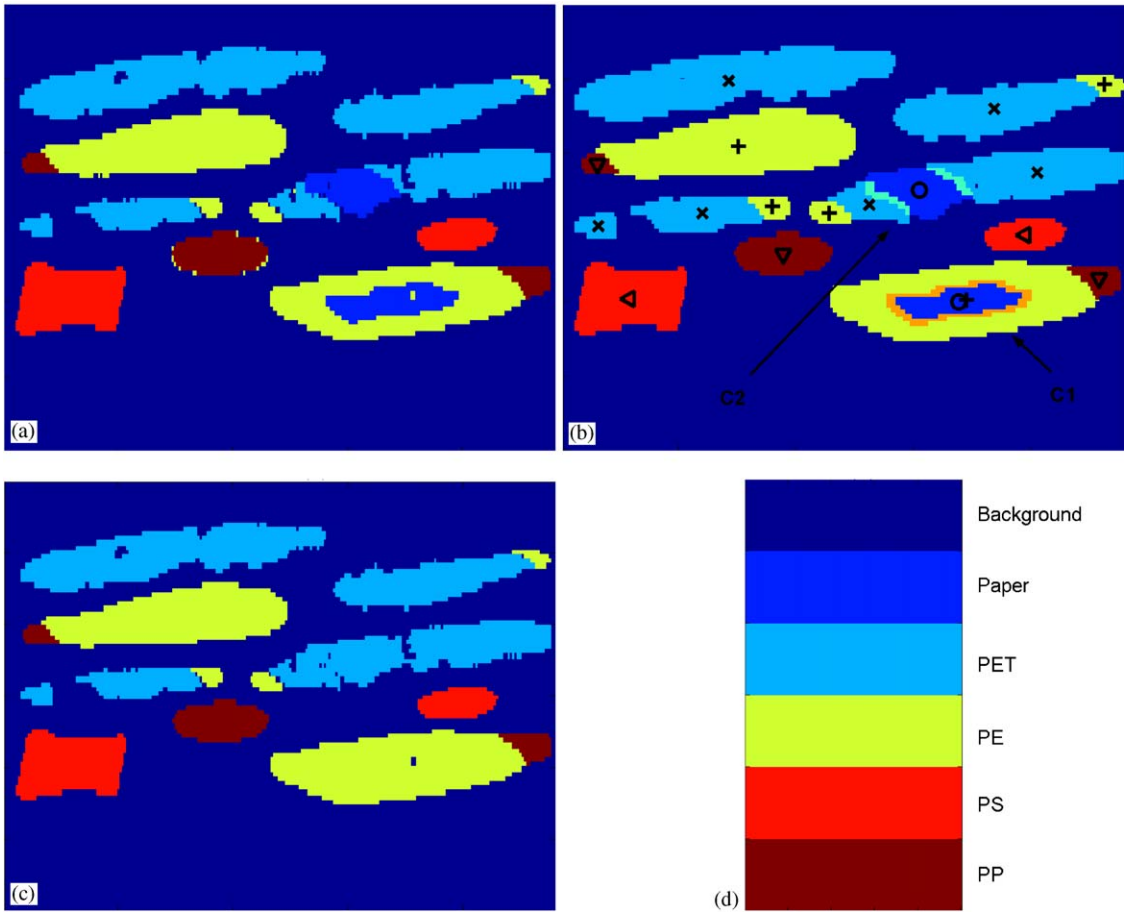

Fig. 5. Classification result (a), dilated classification result (b) with overlaps (orange, cyan), enhanced classification result (c) and the colour mapping (d).

powerful method for industrial sorting applications such as the automated sorting of polymer waste.

Acknowledgements

The co-financing of this research by the "Kärntner Wirtschaftsförderungsfonds" (KWF) is gratefully acknowledged.

References

[1] Burns DA, Ciurczak EW. Handbook of near-infrared analysis, 2nd ed. New York, Basel: Marcel Dekker, Inc.; 2001.
[2] Bearmann GH, Levenson RM, Cabib D, editors. Spectral imaging: basic principles and prospective applications. Dordrecht (Hingham, MA): Kluwer Academic Publishers; 2002.
[3] Hyvärinen T, Herrala E, Dall'Ava A. Direct sight imaging spectrograph: a unique add-on component brings spectral imaging to industrial applications. SPIE Symposium on Electronic Imaging 1998. p. 3302.
[4] Kulcke A, Gurschler C, Spöck G, Leitner R, Kraft A. On-line classification of synthetic polymers using near infrared spectral imaging. Journal of Near-Infrared Spectroscopy 2003;11:71–81.
[5] van der Meer F, De John SM, editors. Imaging spectrometry: basic principles and prospective applications. Dordrecht (Hingham, MA): Kluwer Academic Publishers; 2002.
[6] Bearman GH, Levenson RM, Cabib D, editors. Spectral Imaging: Instrumentation, Applications, and Analysis. SPIE Publications, 2000.
[7] Smith RD, Nelson MP, Treado PJ. Raman chemical imaging using flexible fiberscope technology. Proceedings of the SPIE 2000;3920:14.
[8] Hopkins MF. Four-color pyrometry for metal emissivity characterization. Proceedings of the SPIE 1995;2599:294.
[9] Gat N. Imaging spectroscopy using tunable filters: a review. Proceedings of the SPIE 2000;4056:50.
[10] Bennett CL, Carter MR, Fields DJ, Hernandez J. Imaging Fourier transform spectrometer. Proceedings of the SPIE 1993; 1937:191.
[11] Wadsworth W, Dybwad JP. Proceedings of the SPIE 1999; 3537:54.
[12] Gat N. Spectrometer apparatus. US Pat 1992;5166755.
[13] Hyvarinen T, Herrala E, Dall'Ava A. Proceedings of the SPIE 1998;3302:165.
[14] Abbott JA. Quality measurements of fruits and vegetables. Postharvest and Biology Technology 1995;15:207–25.
[15] Polder G, van der Heijden GWAM, Young IT. Hyperspectral image analysis for measuring the ripeness of tomatoes. ASAE International Meeting, Paper No. 003089, Milwaukee, WI, 2000.

[16] Lawrence KC, Windham WR, Park B, Buhr RJ. Hyperspectral imaging for poultry contaminant detection. NIR News 2001; 12(5):3–6.
[17] von der Heijden GWAM, Polder G, Gevers T. Comparison of multispectral images across the Internet. Proceedings of the SPIE 2000;3964:196–206.
[18] Gurschler C, Serafino G, Spöck G, Del Bianco A, Kraft M, Kulcke A. Spectral imaging for the classification of natural and artificial turquoise samples. Int Conf OPTO, Erfurt 2002. p. 197.
[19] Pekalska E, Duin RPW. Classifiers for dissimilarity-based pattern recognition. In: Sanfeliu A, Villanueva JJ, Vanrell M, Alquezar R, Jain AK, Kittler J, editors. ICPR15, proceedings 15th Int. conference on pattern recognition (Barcelona, Spain, Sep.3–7), pattern recognition and neural networks, Vol. 2. Los Alamitos: IEEE Computer Society Press; 2000. p. 12–6.